

# Convenient One-Pot Formation of 2,3-Dialdehyde Cellulose Beads via Periodate Oxidation of Cellulose in Water

Jonas Lindh,\*<sup>†</sup> Daniel O. Carlsson,<sup>†</sup> Maria Strømme,<sup>†</sup> and Albert Mihranyan\*,<sup>†,‡</sup>

<sup>†</sup>Nanotechnology and Functional Materials, Department of Engineering Sciences, Uppsala University, Box 534, 75121 Uppsala, Sweden

<sup>‡</sup>Division of Materials Science, Luleå University of Technology, 97187 Luleå, Sweden

## Supporting Information

## ■ INTRODUCTION

Formation of cellulose beads was reported for the first time in the early 1950s,<sup>1</sup> and since then, several methods for bead formation have been developed.<sup>2</sup> Cellulose beads have been used in a wide range of applications, such as liquid chromatography as column material, water purification, protein purification, and as a drug delivery vehicle.<sup>3</sup> (For an excellent review on cellulose beads, see Gericke et al.<sup>2</sup> and references therein.)

The preparation of cellulose beads is, however, a tedious multistep process, typically relying on phase inversion and involving the same basic steps: (1) dissolution of the cellulose in a suitable solvent (e.g., organic solvent or ionic liquid), (2) atomization and/or surfactant-aided dispersion, and (3) coagulation and solidification of the droplets formed in an antisolvent (i.e., coagulant solution).<sup>2</sup> Each of these steps may pose problems. Dedicated solvents are required in order to dissolve the cellulose, and chemical modifications of the cellulose are possibly required to facilitate dissolution. Many of the solvents commonly used for this purpose are toxic, flammable, chemically aggressive, and/or expensive. The second step, involving droplet formation of the dissolved cellulose phase, is critical and often requires sophisticated equipment and rigorous control to produce the desired droplet size. Although there are a number of sophisticated methods for droplet formation, formation of small (1–10  $\mu\text{m}$ ) droplets is difficult, and surfactant-aided dispersion techniques are often needed.<sup>4</sup>

Our group has made research efforts toward finding industrial applications of cellulose from the water-polluting green algae *Cladophora* (*Clad.*).<sup>5</sup> Apart from its high chemical inertness, which is believed to be related to the relatively high thickness of *Clad.* cellulose elementary fibrils (20–30 nm),<sup>6</sup> the cellulose from *Clad.* also features other properties such as a high crystallinity (95%; crystallinity index<sup>5i,7</sup> determined by XRD), high specific surface area (SSA) up to 170  $\text{m}^2 \text{ g}^{-1}$ , and a mesoporous structure.<sup>8</sup>

An attempt to produce highly oxidized *Clad.* 2,3-dialdehyde cellulose (DAC) via periodate oxidation led to the surprising discovery of a one-pot procedure for the formation of DAC beads in water. Sodium periodate-mediated oxidation of cellulose is known to selectively oxidize the vicinal hydroxyl groups in the C2 and C3 positions to the corresponding aldehydes with the concomitant cleavage of the C2–C3 bond and is one of the most potent methods for cellulose modification. The reaction produces DAC, which has a number

of interesting applications in, for example, protein immobilization,<sup>9</sup> chromatography,<sup>10</sup> drug delivery,<sup>3,11</sup> and graft copolymerization.<sup>12</sup>

Periodate oxidation of highly crystalline cellulose (e.g., cellulose from *Clad.*) has been previously investigated by Kim and Kuga.<sup>13</sup> Although a high concentration of periodate, corresponding to 10.7 equiv of sodium metaperiodate per anhydroglucose unit, and long reaction times of up to 260 h were employed, the degree of oxidation did not exceed 30%.<sup>13</sup>

In this note, we show that, contrary to data reported by Kim and Kuga,<sup>13</sup> it is possible to achieve complete oxidation of the 2,3-hydroxyl groups in *Clad.* cellulose and that the morphological and structural properties can be tailored to either retain its nanofibrous texture, while ensuring a high degree of oxidation, or to produce fully oxidized DAC spherical beads.

To obtain DAC, we investigated the effect of different pH on periodate oxidation by performing the reaction in three different batches (i.e., at pH 5.5, pH 4.5, and under unbuffered conditions ( $\text{pH} \leq 4.5$ )). Subsequently, aliquots were withdrawn from the reaction mixtures after 24, 48, 72, 96, 168, and 240 h and analyzed as described below. The amount of sodium metaperiodate was fixed to 5 equiv per anhydroglucose unit.

## ■ EXPERIMENTAL SECTION

**Materials.** Nanocellulose from *Clad.* algae was provided by FMC Biopolymer. Sodium metaperiodate, hydroxylamine hydrochloride, sodium borohydride, Oxone (potassium peroxymonosulfate), and other chemicals used were of analytical or reagent grade and were used as received. Deionized water was used throughout the experimental procedures.

**Methods. Preparation of DAC.** Three different batches were prepared with respect to the pH of the reaction medium: water (unbuffered), acetate buffer at pH 4.5, and acetate buffer at pH 5.5. *Clad.* cellulose, 12 g in 900 mL of water or acetate buffer (pH 4.5 or pH 5.5), was mixed with 79 g of sodium metaperiodate (about 5 mol per mol of anhydroglucose units) dissolved in 900 mL of the same medium as the cellulose. The periodate-containing reaction mixture was carefully wrapped in aluminum foil to avoid light exposure, and 180 mL of 1-propanol was added to the reaction mixture to serve as a radical scavenger.<sup>14</sup> The reaction mixture was vigorously stirred at room temperature in the dark for 10 days. Aliquots were withdrawn after 24, 48, 72, 96, 168, and 240 h (300 mL each time). The withdrawn aliquots were immediately quenched via the addition of

Received: February 25, 2014

Revised: April 3, 2014

Published: April 7, 2014

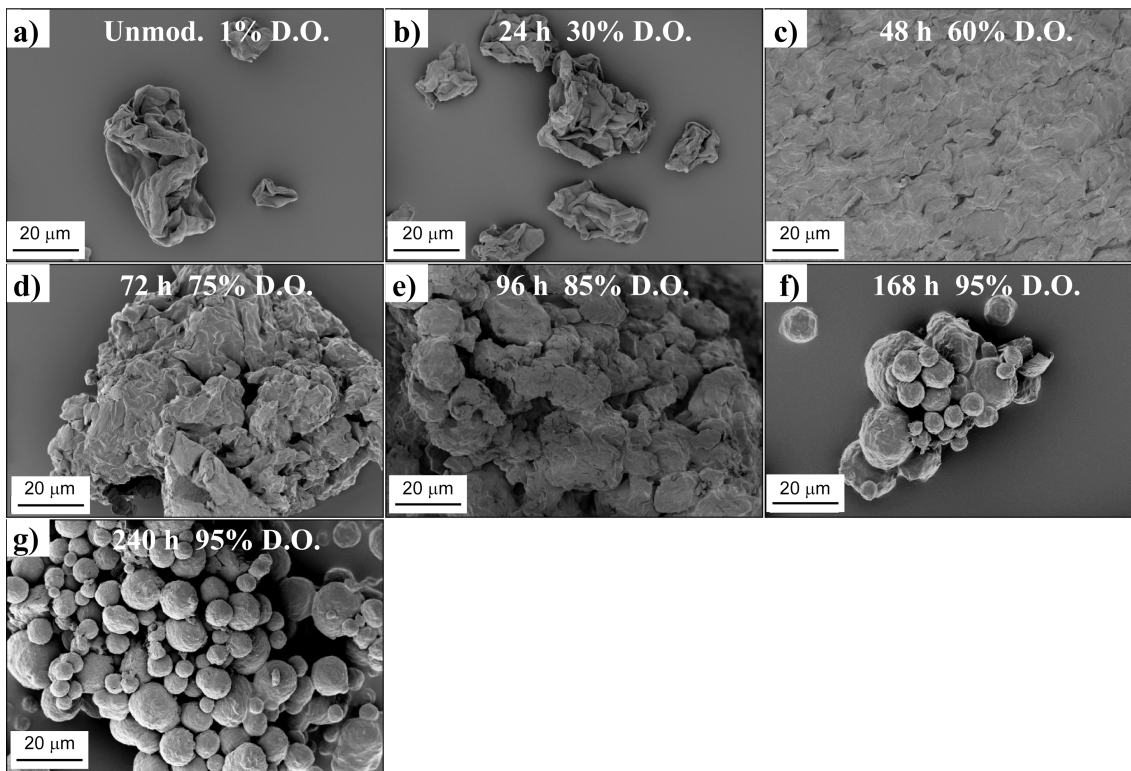


**Figure 1.** Scanning electron micrographs of (a) unmodified *Cladophora* cellulose and (b–g) *Cladophora* DAC oxidized at pH 5.5 for 24–240 h. Scale bar: 20  $\mu$ m.

ethylene glycol and washed repeatedly with water to provide pure DAC.

**Determination of Aldehyde Content.** The DAC samples were transformed to aldoximes via Schiff base reactions with hydroxylamine according to a literature procedure<sup>13</sup> and were analyzed for elemental composition (C, H, and N). To a stirred 100 mL RB-flask was added never-dried DAC (corresponding to a dry weight of 100 mg), 40 mL of acetate buffer (pH 4.5), and 1.65 mL of hydroxylamine solution (aqueous, 50 wt %). The reaction mixture was stirred at room temperature for 24 h. The product was thoroughly washed with water and dried under reduced pressure prior to elemental analysis. The term degree of oxidation (D.O.) represents the ratio of 2,3-alcohols in the anhydroglucoside units that has been transformed into their corresponding aldehydes. The highest degree of oxidation (i.e., 100%) corresponds to all anhydroglucoside units being converted to the corresponding noncyclic 2,3-dialdehyde structure, which would correspond to approximately 12.5 mmol of aldehyde groups per gram of cellulose.

**Reductive Amination of 1,7-Diaminoheptane to DAC Beads.** To a 100 mL RB-flask was added never-dried DAC (corresponding to a dry weight of 100 mg), 40 mL of phosphate buffer (pH 7.0), and 40 mg of 1,7-diaminoheptane. The reaction mixture was stirred at room temperature for 24 h. The product was washed with water. The resulting imine product was treated with sodium borohydride (1.2 equiv), and reduction was performed over 2 h. The crude product was washed with water followed by EtOH and dried in air.

**Scanning Electron Microscopy.** Scanning electron micrographs were recorded with a LEO1550 field-emission SEM instrument (Zeiss, Germany). Samples were mounted on aluminum stubs by means of double-sided adhesive carbon tape and sputtered with Au/Pd to reduce charging effects.

**X-ray Diffraction.** An X-ray diffractometer with Bragg–Brentano geometry (Cu K $\alpha$  radiation;  $\lambda = 1.54 \text{ \AA}$ ) was used (D5000, Siemens/Bruker, Germany). The crystallinity index was calculated as previously described.<sup>5,6,7</sup>

**NMR.** All NMR experiments were performed on a Varian Inova-600 operating at 14.7 T and equipped with a 3.2 mm solid-state probe.

Measurements were conducted at 301 K with a MAS spinning rate of 15 kHz. The CP/MAS  $^{13}\text{C}$  NMR spectra were recorded using a cross-polarization pulse sequence followed by proton decoupling during acquisition. Acquisition parameters included a 2.9  $\mu\text{s}$   $^1\text{H}$  90° pulse, 1200  $\mu\text{s}$  contact time, 25 ms acquisition time, and 54 s recycle delay to allow for complete thermal equilibrium.

## RESULTS AND DISCUSSION

The SEM micrographs in Figure 1 show DAC samples prepared in buffered solution at pH 5.5. Drastic morphological changes induced by periodate oxidation are clearly visible: as the degree of oxidation increases, the cellulose texture becomes more compact and, at the highest degree of oxidation, spherically shaped beads are formed with a diameter generally ranging between 1 to 20  $\mu$ m, according to the SEM images. Whereas periodate oxidation of cellulose has been reported to generate more compact cellulose structures,<sup>15</sup> this is the first time that the formation of spherical beads has been reported. To verify that the oxidation itself was responsible for the morphological changes, additional experiments excluding any additives, such as ethylene glycol in the quenching step or 1-propanol as the radical scavenger, were performed; all of these experiments resulted in bead formation. Furthermore, the washing step was examined by exchanging the centrifugation step with filtration, which also produced beads. The effect of the agitation of the reaction mixture was examined by replacing the originally employed magnetic stirring with orbital shaking, which also provided beads. The reduced stiffness of the fibers as a result of the glucose ring-opening, changes in fiber dimensions, and formation of inter- and intrafibrillar hemiacetal cross-links are all plausible factors contributing to the observed morphological transitions.

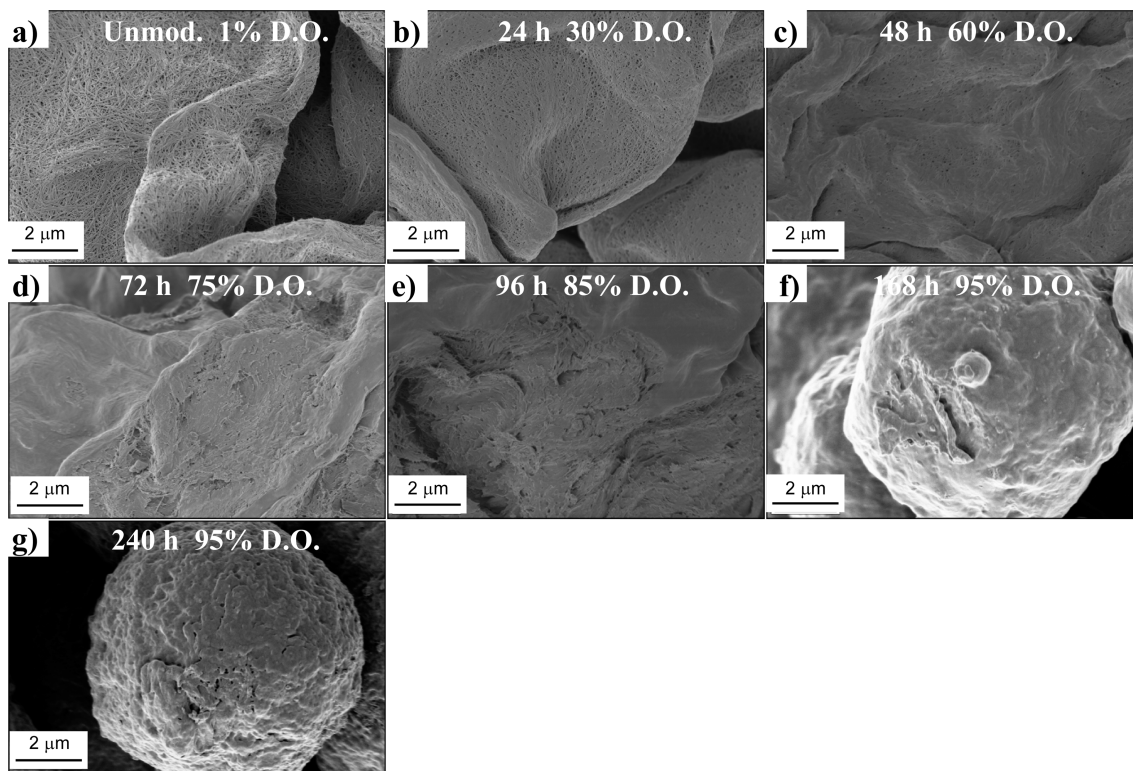


**Figure 2.** SEM images of (a) unmodified *Cladophora* cellulose and (b–g) *Cladophora* DAC oxidized at pH 5.5 for 24–240 h. Scale bar: 2  $\mu$ m.

Somewhat surprisingly, this method of DAC bead formation was found to be ineffective for other (less crystalline) sources of cellulose (i.e., microfibrillated cellulose (MFC) and micro-crystalline cellulose (MCC)), which did not form spherical shapes even after extensive oxidation but rather formed compact materials with smooth surfaces and no visible fibers. Chitosan of both high and low molecular weight was also oxidized, but no beads were formed for such polymers, and only traces of solid material could be recovered.<sup>16</sup>

SEM images of DAC samples prepared at pH 4.5 and under unbuffered conditions ( $\text{pH} \leq 4.5$ ) show similar morphologies as those in Figure 1, with the noticeable difference being that the fibers are disintegrated already at a lower D.O. The observed disintegration is further supported by crystallinity data of the samples (see Figure 3 and the following discussion).

SEM images at higher magnification show that as the D.O. increases the nanofibrous texture of cellulose progressively disappears (Figure 2). The nanofibers are distinguishable up to a D.O. of 60%, whereas more highly oxidized samples form smoother and more compact structures. The deterioration of fibers into a nonporous mass following the periodate oxidation was verified by a  $\text{N}_2$  gas adsorption analysis (Supporting Information, Figure S1). The  $\text{N}_2$  BET analysis data show that the SSA decreases by as much as 2 orders of magnitude from 102 to 0.2–0.9  $\text{m}^2 \text{ g}^{-1}$  when the D.O. increases from 0 to 60%.

On the basis of the XRD profiles of the samples (Figure 3a), the starting material features a crystallinity index of 95%. Following periodate oxidation, the cellulose crystallinity decreases with time, and it decreases more rapidly at lower pH (Figure 3b). The sample prepared in the unbuffered solution, where the pH decreased from an initial value of 4.5 to 3.8 after 240 h, is completely amorphous after 72 h of oxidation, whereas for the oxidation performed at pH 5.5, the sample is rendered completely amorphous after only 240 h of

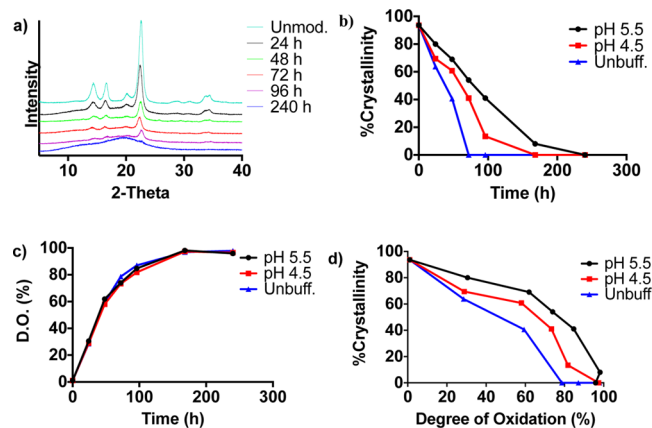


**Figure 3.** (a) Changes in the X-ray diffraction pattern induced by periodate oxidation at pH 5.5. Top to bottom: unmodified *Clad.* cellulose, 24, 48, 72, 96, and 240 h. (b) Changes in crystallinity as a function of reaction time of DAC samples oxidized at pH 5.5 (circles), pH 4.5 (squares), and in unbuffered water (triangles). (c) D.O. as a function of time for DAC samples oxidized at pH 5.5 (circles), pH 4.5 (squares), and in unbuffered water (triangles). (d) Changes in crystallinity with increasing D.O. for DAC samples oxidized at pH 5.5 (circles), pH 4.5 (squares), and in unbuffered water (triangles). The solid lines in panels b–d serve as guides to the eye.

oxidation. Interestingly, the reaction yield was not affected by the pH of the reaction mixture, and both the unbuffered and the pH 5.5 conditions provided good yields of pure product (77% after 240 h of oxidation).

The degree of cellulose oxidation increased almost independently of the pH of the reaction mixture (Figure 3c), which is in agreement with previous studies.<sup>17</sup> When comparing the samples oxidized at different pH, it is evident that at the same D.O. the samples oxidized at pH 5.5 maintain higher

cellulose crystallinity than the samples oxidized under more acidic conditions (Figure 3d). This observation is of practical importance because it is often desirable to maintain cellulose crystallinity and nanofibrous texture, which strongly influence the mechanical properties of cellulose. It has recently been reported that a pH > 4 would inhibit the periodate oxidation of cellulose,<sup>18</sup> a conclusion that is contradicted by our findings. The decrease in cellulose crystallinity and increase in D.O. is accompanied by a decrease in true density. The decrease in true density from 1.64 g cm<sup>-3</sup> for the starting material to about 1.48 g cm<sup>-3</sup> for fully amorphous DAC reflects the disruption of the hydrogen-bond network (Supporting Information, Figure S2).

The loss of crystallinity with increasing D.O. is further manifested in solid-state <sup>13</sup>C NMR spectra (Figure 4). As in

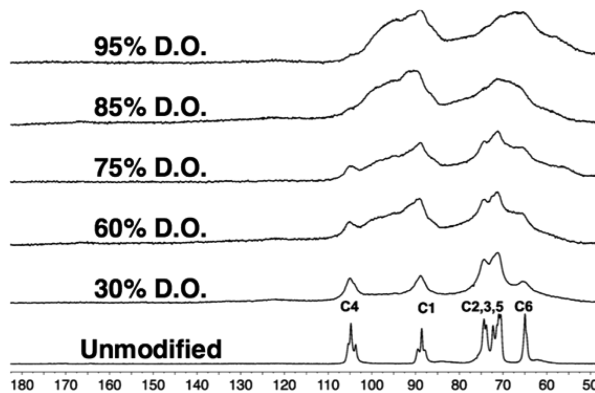


**Figure 4.** <sup>13</sup>NMR spectra of (from the bottom) unmodified cellulose, 30, 60, 75, 85, and 95% D.O.

previous NMR studies of DAC, the expected carbonyl signal at 175–180 ppm is not observed even at the highest degrees of oxidation, which can be explained by the formation of hemiacetals.<sup>13</sup>

Because the presented method for DAC bead formation consumes large amounts of periodate, it is of interest to regenerate the used periodate. On the basis of a published procedure,<sup>19</sup> the liquid content of the reaction mixture and the water used for washing the product were collected after completing a 240 h periodate oxidation. The liquid volume was reduced via rotary evaporation, and the low-cost oxidant Oxone was used to reoxidize the consumed periodate. The periodate precipitated during the reaction and was then recovered by filtration. Without any optimization, a recovery of 70% was achieved.

The beads in Figure 1 have a smooth and nonporous texture, which is probably related to the drying procedure. To generate beads with a porous texture, we performed reductive amination using never-dried DAC beads and a diamine (1,7-diaminoheptane). As seen in Figure 5a, the amine-grafted bead has a porous texture, and BET measurements revealed a SSA of 20 m<sup>2</sup> g<sup>-1</sup> (i.e., up to a 100-fold increase in SSA compared to the unfunctionalized DAC beads). Remarkably, when performing the reductive elimination with hydroxylamine, the resulting functionalized DAC beads show a very smooth texture and a perfectly spherical shape (Figure 5b).

## CONCLUSIONS

Under the presented conditions for extensive periodate oxidation of highly crystalline cellulose, great morphological modifications of cellulose can be achieved. This facile one-pot procedure in water does not require organic solvents or ionic liquids to dissolve cellulose, it avoids the use of regenerating coagulant solutions and surfactants or other surface active dispersion aids, and it does not employ spraying, atomization, or any other droplet-forming equipment, thereby significantly facilitating production. Moreover, the produced beads have a degree of oxidation of 80–100%, providing a multitude of possibilities for further modifications by utilizing the aldehyde groups to obtain functionalized beads with high functional group density and high yield. A number of useful applications of the DAC beads via simple imine formation can be hypothesized, such as protein immobilization and amine scavenging, affinity chromatography columns for peptide purification, and immunoabsorbents, among others. There are, to the best of our knowledge, no previously known ways of producing cellulose beads via periodate oxidation on its own.

## ASSOCIATED CONTENT

### S Supporting Information

Data describing the specific surface and true density of the materials. This material is available free of charge via the Internet at <http://pubs.acs.org>.

## AUTHOR INFORMATION

### Corresponding Authors

\*(J.L.) E-mail: [jonas.lindh@angstrom.uu.se](mailto:jonas.lindh@angstrom.uu.se).

\*(A.M.) E-mail: [albert.mihranyan@angstrom.uu.se](mailto:albert.mihranyan@angstrom.uu.se).

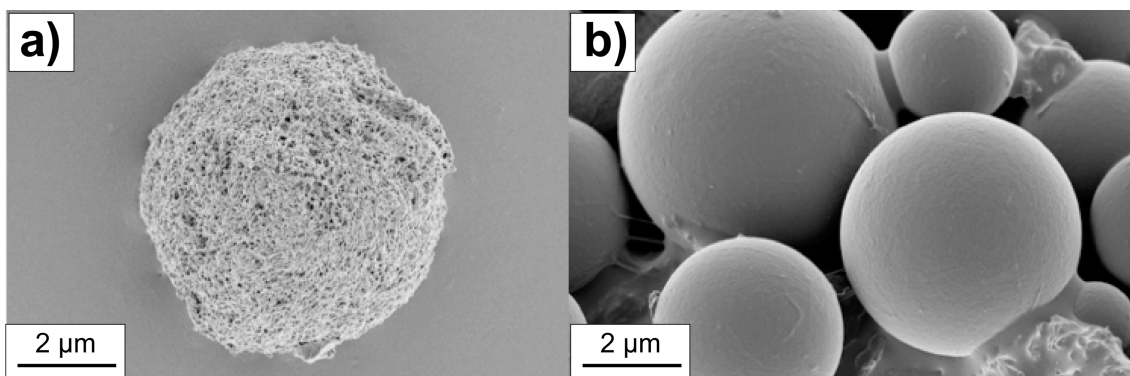


**Figure 5.** (a) DAC bead grafted with 1,7-diaminoheptane and (b) DAC beads grafted with hydroxylamine.

**Author Contributions**

The manuscript was written through contributions of all authors. All authors have given approval to the final version of the manuscript.

**Notes**

The authors declare no competing financial interest.

**ACKNOWLEDGMENTS**

The Swedish NMR Centre is acknowledged for spectrometer time, and Dr. Diana Bernin is acknowledged for sample preparation and for performing the NMR experiments. The Swedish Research Council (VR) and the Göran Gustafsson Foundation are gratefully acknowledged for their financial support. A.M. is a Wallenberg Academy Fellow and thanks the Knut and Alice Wallenberg Foundation for their support.

**REFERENCES**

- (1) O'Neill, J. J.; Reichardt, E. P. U.S. Patent 2,543,928, 1951.
- (2) Gericke, M.; Trygg, J.; Fardim, P. *Chem. Rev.* **2013**, *113*, 4812–4836.
- (3) Wolf, B.; Finke, I. *Pharmazie* **1992**, *47*, 121–125.
- (4) Thuemmler, K.; Fischer, S.; Feldner, A.; Weber, V.; Ettenauer, M.; Loth, F.; Falkenhagen, D. *Cellulose* **2011**, *18*, 135–142.
- (5) (a) Strømme, M.; Mihranyan, A.; Ek, R. *Mater. Lett.* **2002**, *57*, 569–572. (b) Mihranyan, A.; Andersson, S. B.; Ek, R. *Eur. J. Pharm. Sci.* **2004**, *22*, 279–286. (c) Mihranyan, A.; Edsman, K.; Strømme, M. *Food Hydrocolloids* **2007**, *21*, 267–272. (d) Nyström, G.; Razaq, A.; Strømme, M.; Nyholm, L.; Mihranyan, A. *Nano Lett.* **2009**, *9*, 3635–3639. (e) Razaq, A.; Nyström, G.; Strømme, M.; Mihranyan, A.; Nyholm, L. *PLoS One* **2011**, *6*, e29243-1–e29243-9. (f) Ferraz, N.; Carlsson, D. O.; Hong, J.; Larsson, R.; Fellström, B.; Nyholm, L.; Strømme, M.; Mihranyan, A. *J. R. Soc., Interface* **2012**, *9*, 1943–1955. (g) Ferraz, N.; Leschinskaya, A.; Toomadj, F.; Fellström, B.; Strømme, M.; Mihranyan, A. *Cellulose* **2013**, *20*, 2959–2970. (h) Gelin, K.; Mihranyan, A.; Razaq, A.; Nyholm, L.; Strømme, M. *Electrochim. Acta* **2009**, *54*, 3394–3401. (i) Mihranyan, A.; Llagostera, A. P.; Karmhag, R.; Strømme, M.; Ek, R. *Int. J. Pharm.* **2004**, *269*, 433–442. (j) Nyholm, L.; Nyström, G.; Mihranyan, A.; Strømme, M. *Adv. Mater.* **2011**, *23*, 3751–3769. (k) Razaq, A.; Nyholm, L.; Sjödin, M.; Strømme, M.; Mihranyan, A. *Adv. Energy Mater.* **2012**, *2*, 445–454. (l) Hua, K.; Carlsson, D. O.; Ålander, E.; Lindström, T.; Strømme, M.; Mihranyan, A.; Ferraz, N. *RSC Adv.* **2014**, *4*, 2892–2903. (m) Carlsson, D. O.; Hua, K.; Forsgren, J.; Mihranyan, A. *Int. J. Pharm.* **2014**, *461*, 74–81.
- (6) (a) Wickholm, K.; Larsson, P. T.; Iversen, T. *Carbohydr. Res.* **1998**, *312*, 123–129. (b) Okita, Y.; Saito, T.; Isogai, A. *Biomacromolecules* **2010**, *11*, 1696–1700.
- (7) Segal, L.; Creely, J.; Martin, A.; Conrad, C. *Text. Res. J.* **1959**, *29*, 786–794.
- (8) Mihranyan, A.; Esmaeili, M.; Razaq, A.; Alexeichik, D.; Lindström, T. *J. Mater. Sci.* **2012**, *47*, 4463–4472.
- (9) (a) Gurvich, A. E.; Lechtzind, E. V. *Mol. Immunol.* **1982**, *19*, 637–640. (b) Aniulyte, J.; Liesiene, J.; Niemeyer, B. *J. Chromatogr. B: Anal. Technol. Biomed. Life Sci.* **2006**, *831*, 24–30.
- (10) Kim, U. J.; Kuga, S. *Cellulose* **2000**, *7*, 287–297.
- (11) Dash, R.; Ragauskas, A. *J. RSC Adv.* **2012**, *2*, 3403–3409.
- (12) Dash, R.; Elder, T.; Ragauskas, A. *J. Cellulose* **2012**, *19*, 2069–2079.
- (13) Kim, U. J.; Kuga, S.; Wada, M.; Okano, T.; Kondo, T. *Biomacromolecules* **2000**, *1*, 488–492.
- (14) Painter, T. *J. Carbohydr. Res.* **1988**, *179*, 259–268.
- (15) Potthast, A.; Kostic, M.; Schiehser, S.; Kosma, P.; Rosenau, T. *Holzforschung* **2007**, *61*, 662–667.
- (16) Vold, I. M. N.; Christensen, B. E. *Carbohydr. Res.* **2005**, *340*, 679–684.
- (17) Varma, A. J.; Kulkarni, M. P. *Polym. Degrad. Stab.* **2002**, *77*, 25–27.
- (18) Liu, X.; Wang, L.; Song, X.; Song, H.; Zhao, J. R.; Wang, S. *Carbohydr. Polym.* **2012**, *90*, 218–223.
- (19) Besemer, A. U.S. Patent 6,620,928 B2, 2003.